



Experimental and Numerical Analysis of an Outward Opening Injector Pintle Dynamics

Rodrigo Eguluz, Luke Stover, Tommy Powell, Tiago Costa, Alexander Kopache, and Peter Hartman

LiquidPiston Inc.

Joonsik Hwang Mississippi State University

Alexander Shkolnik LiquidPiston Inc.

Citation: Eguluz, R., Stover, L., Powell, T., Costa, T. et al., "Experimental and Numerical Analysis of an Outward Opening Injector Pintle Dynamics," SAE Technical Paper 2023-01-1810, 2023, doi:10.4271/2023-01-1810.

Received: 01 Jun 2023

Revised: 01 Sep 2023

Accepted: 5 Sep 2023

Abstract

Direct injection strategies have been successfully used on spark ignited internal combustion engines for improving performance and reducing emissions. Among the different technologies available, outward opening injectors seem to have found their place in renewable applications running on gaseous fuels, including natural gas or hydrogen, as well as in a few specific liquid fuel applications.

In order to understand the key operating principles of these devices, their limitations and the resulting sprays, it is necessary to accurately describe the pintle dynamics. The pintle's relative position with respect to the injector body defines the internal flow geometry and therefore the injection rates and spray characteristics.

In this paper both numerical and experimental investigations of the dynamics of an outward opening injector pintle

have been carried out. The injector average flow rates and instantaneous pintle position have been experimentally measured at a variety of pressures and injection durations using air as the working fluid. In addition to the experimental measurements, the injector internals were thoroughly measured and characterized so that a high-fidelity numerical model could be assembled.

A multi-physics model featuring a simplified electromagnetic representation of the injector solenoid and a spring-mass-damper system for the pintle dynamics integrated with a 1-dimensional computational fluid dynamics description of the internal flow using two-way fluid-structure-interaction coupling was developed in the commercial software GT-Suite. The model is capable of accurately predicting the pintle position and average flow rates, at a variety of conditions, using working fluid pressure and injector current profile as the only inputs.

Introduction

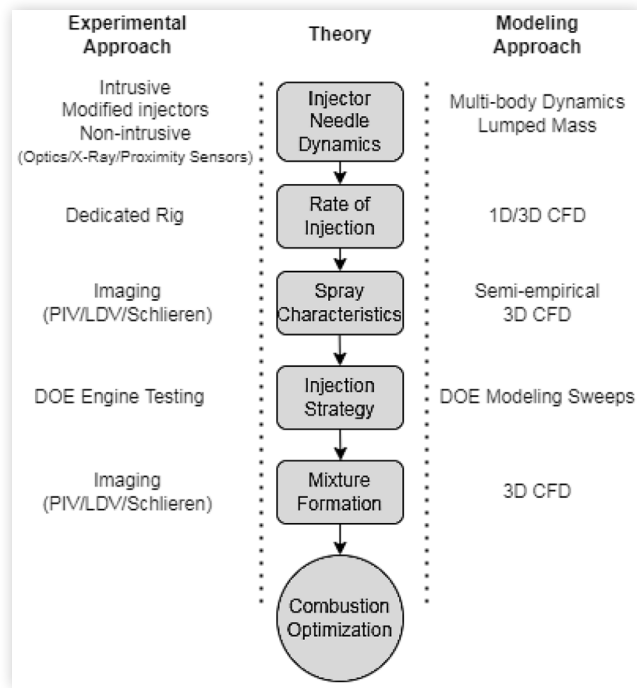
One of the main aspects to optimizing combustion in existing or new engine designs is mixture formation. Modeling-based approaches are critical for guiding design changes and improved control strategies, although they are not a replacement for experimental methods. The key aspects involved in the formation of air-fuel mixture and therefore combustion optimization are outlined in [Figure 1](#).

Injector pintle instantaneous position with respect to the injector seat is one of the most important aspects affecting the injection process since it defines the geometry of the flow problem [1], and the use of a mismatched lift profile can result in cascading errors throughout the entire simulation of mixture formation. While injection dynamics and mass flow rates are predictable at steady-state conditions, pintle bounce has been shown to cause significant non-linearities in the injected mass of fuel due to the rapid change in the flow area

and geometry inside the injector. It was found that these non-linearities were most significant at shorter injection dwells due to the bounce events still being damped out [2, 3]. Unfortunately, pintle bounce will also cause significant issues at elevated engine speeds, where injection events must occur in a shorter amount of time. Injector pintle bounce can also increase emissions due to poor sealing of the injector or over-fueling, contributing to poor combustion quality, and greater smoke or hydrocarbon emissions [2, 3].

Most of the present body of injector modeling work focuses on spray characteristics such as spray penetration, cone angle, and droplet size [4], or rate of injection [5]. These simulations often rely on experimental pintle lift data if available, modeled as a trapezoidal pulse, or in some cases, fixed position and/or imposed ROI data from experiments or simpler models [4, 6, 7, 8, 9]. Given the transient effects of needle bounce on injector flow, this unfortunately means these

FIGURE 1 Path to combustion optimization through injection process.



assumptions limit the predictiveness of the injector and spray models.

While inward opening injectors are well documented [5, 10] and modeled outward opening pintle injectors have received less attention in the automotive industry, due to their niche applications [7, 8, 9, 11]. The growing interest in gaseous and multi-phase fuel applications with low-carbon intensity has brought some focus on outward opening pintle injectors.

This paper covers the experimental and analytical methods used to assess the influence of different operation parameters on the injector pintle dynamics. A numerical model capable of predicting the instantaneous injector pintle position was developed, thus providing additional insight on the operating principles of this kind of injector and better boundary conditions for more advanced numerical models such as 3D flow and spray simulations. First, injector physical dimensions and electromechanical characteristics were measured to provide a simplified representation of the solenoid and pintle-spring-seat systems. Experimental data of instantaneous injector current and lift were recorded under “dry” conditions, i.e., with no pressurized working fluid, and used to tune the initial model. To support the fluid flow model, a coefficient of discharge curve was characterized at different working fluid pressures by holding pintle lift constant. Air was the selected fluid. Next, air pressure sweeps were conducted in normal injector operation, to study the two-way fluid-structure-interaction and add it to the model. This scaffolding approach between experimental testing and model tuning resulted in a model capable of accurately predicting pintle lift with injector current and air pressure as the only inputs.

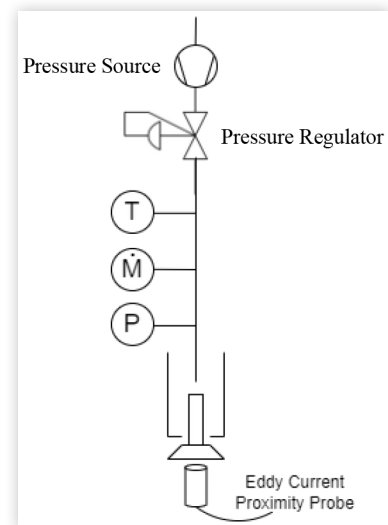
Experimental Setup

The injector used in this study is an outward opening pintle valve with a narrow cone angle. Maximum pintle lift of approximately 0.22 mm was measured with a dial indicator. The injector was disassembled and internal components such as pintle assembly and the spring were weighed and characterized. The injector was ground along the axial plane in order to expose the interior geometry. Using a combination of Keyence VR optical profilometer scans and manual measurements, the inner geometry was measured to within 0.1 micrometers.

The test stand (Figure 2) uses a stock OEM injector housing with the injector described earlier. Air supply for the experiment was sourced from the laboratory’s shop compressor, regulated to maintain the target pressure within the range of 1 to 6 BarG. Air flow rates were measured using an Omega FMA1842 0-100 slpm flow meter. Type K thermocouples were employed to monitor the air rail temperature. Upstream of the injector housing, Kistler 4007 absolute pressure transducers were positioned to record instantaneous pressure data. For pintle lift measurement, a PU-05 AEC proximity sensor was mounted in a custom bracket and calibrated to operate at a consistent 1 mm distance from the nozzle. Injector driving current measurements used a Tektronix A622 current clamp with a sensitivity of 100 mv/A.

Data acquisition and injector control were handled by a Driven tower, a system commissioned by Vieletech Inc., which is equipped with a National Instruments NI-9751 injector module. The voltage for the direct injector driver ranged from 14 to 24 volts, supplied by an external power source. Injector current, proximity probe readings, and absolute pressure were recorded at 38 kHz, while temperature and flow rates were down-sampled to 1 Hz. Each experimental run involved collecting data for 200 simulated engine cycles.

FIGURE 2 Representation of experimental set-up with temperature (T), mass flow (M), and pressure (P) measurements



For studying the system electrodynamics with no air flow and its effects on the opening rate of the injector, a full factorial DOE with a total of 20 experiments was used. Injector pulse width durations were swept from 1-2 ms in 5 levels, with higher fidelity on the lower durations to capture the transition to non-linear condition (1,1.1,1.25,1.5, and 2 ms) while high voltage targets were swept in 4 levels (14, 18, 20 and 24 volts). For assessing the effect of air pressure on the injector's opening rate, an experimental matrix similar to the one used on the electrodynamic study was chosen. Same pulse width durations were kept while limiting the high voltage targets to only 2 levels (14 and 20 volts) in order to reduce the number of tests. Air pressures were swept from 1 to 6 BarG.

Measuring the coefficient of discharge used the same hardware and instrumentation for flow tests, apart from the proximity probe being replaced by a set screw, loosely based on the procedure followed on [12]. The screw was set to various lengths using feeler gauges to define the maximum pintle lift. The direct injector driver was substituted by a constant current power supply delivering 2.5 amps to maintain steady opening for CD determination. Flow rates, pressure and temperature were recorded at 1 Hz. After setting the maximum pintle lift, the injector was held open by constant current and pressure was swept down in 1 bar increments.

Numerical Modeling Methodology

Following a similar approach employed by other authors [1, 13, 14], the injector model is divided into three distinct components: the pintle, the flow path, and the solenoid.

In this study, the pivotal component is the pintle, which is considered rigid. Its dynamics are modeled using a single lumped mass, attached to a spring, which represents the actual spring within the injector assembly, and a damper. The damper represents both internal friction losses and viscous damping due to fluid squish within the injector. Additionally, end-stops are incorporated into the model to restrict the pintle's range of motion, just like the injector seats do.

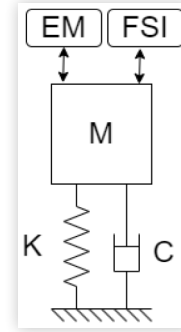
The forces acting on this single mass include electromagnetic (EM) forces derived from the solenoid and forces exerted by the working fluid arising from fluid-structure interaction (FSI). Figure 3 provides a visual representation of this model concept.

Equation (1), the damped oscillator equation, describes the needle dynamics and integration over time provides the instantaneous needle position. The right-hand side of the equation concentrates the external forces acting on the pintle stemming from the solenoid action and the FSI forces. On the left-hand side 3 terms can be observed, one for the inertial forces, one for the frictional losses and damping forces and one for the spring action.

$$m \cdot \ddot{x}(t) + c(x) \cdot \dot{x}(t) + k(x) \cdot x(t) = F(t, x) \quad (1)$$

Both the pintle mass m and spring constant k are known since they are measured when the injector is disassembled.

FIGURE 3 Simplified system representation of injector internals for modeling its dynamics.



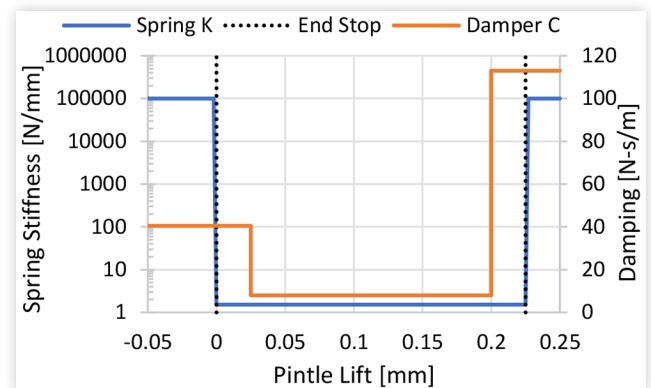
The damping constant c is considered a tuning parameter as experimental characterization in this context is complex and outside the scope of this paper. Note that in equation (1) both k and c are expressed with a dependance on the pintle position x . While both are linear and constant during the needle's main range of motion, near the end-stops these values are adjusted to account for the increased viscous damping and the contact that occurs when the pintle approaches the injector seats. Some compliance to the seats is added in the form of a very stiff spring. Figure 4 shows the values used for these constants during the pintle's full range of motion.

To obtain the FSI forces, fluid flow needs to be resolved. In this case the flow is considered unidimensional and compressible. The flow path can be modeled as a series of 1D pipe elements, and 0D elements such as orifices and emptying-filling volumes. Pressures and friction losses on each of the flow elements are computed and the resulting forces acting on the pintle are obtained. Note that as the pintle moves, some sections of the fluid domain will change their geometry, and this needs to be accounted for when solving the flow problem (FSI).

The pipe elements can be described using the unidimensional flow Euler equations (2-5) [11, 15, 16]:

$$\frac{\partial \rho A}{\partial t} + \frac{\partial \rho u A}{\partial x} = 0, \quad (2)$$

FIGURE 4 Effective spring stiffness and damper constants as a function of pintle position.



$$\frac{\partial \rho u A}{\partial t} + \frac{\partial \rho u^2 A}{\partial x} = -A \frac{\partial P}{\partial x}, \quad (3)$$

$$\frac{\partial EA}{\partial t} + \frac{\partial u(E+p)A}{\partial x} = -p \frac{\partial A}{\partial t}, \quad (4)$$

$$E = \frac{p}{\gamma} + \frac{1}{2} \rho u^2 \quad (5)$$

Where x is the spatial coordinate in the flow direction, t denotes time, A the cross-section area, ρ the density, u the flow velocity, p the pressure, E the total energy and γ is the specific heat ratio.

Small flow passages and orifices follow the isentropic orifice equations [16]. Equation (6) defines the critical pressure ratio. If the pressure ratio $\frac{p_T}{p_0}$ is less than the critical pressure ratio, the flow is said to be choked and equation (8) gives the flow rate, otherwise equation (7) should be used to compute the flow rate.

$$\frac{p_T}{p_0} = \left(\frac{2}{\gamma - 1} \right)^{\frac{\gamma}{\gamma - 1}} \quad (6)$$

$$\dot{m} = \frac{C_D A_T p_0}{\sqrt{RT_0}} \left(\frac{p_T}{p_0} \right)^{\frac{1}{\gamma}} \sqrt{\frac{2\gamma}{\gamma - 1} \left[1 - \left(\frac{p_T}{p_0} \right)^{\frac{\gamma - 1}{\gamma}} \right]} \quad (7)$$

$$\dot{m} = \frac{C_D A_T p_0}{\sqrt{RT_0}} \gamma^{\frac{1}{2}} \left(\frac{2}{\gamma + 1} \right)^{\frac{\gamma + 1}{2(\gamma - 1)}} \quad (8)$$

Where p_T denotes the pressure at the orifice throat, p_0 the pressure upstream the orifice, C_D the orifice discharge coefficient, A_T the orifice geometric area, R is the ideal gas constant and T_0 is the temperature upstream the orifice.

Emptying-filling volume equations can be derived from the mass conservation equation, the equation of state for ideal gases $pV = mRT$ and the first principle of thermodynamics for open systems [16]. These result in a series of differential equations (9-11) that define the evolution of pressure, temperature, and mass within the volume with respect to time.

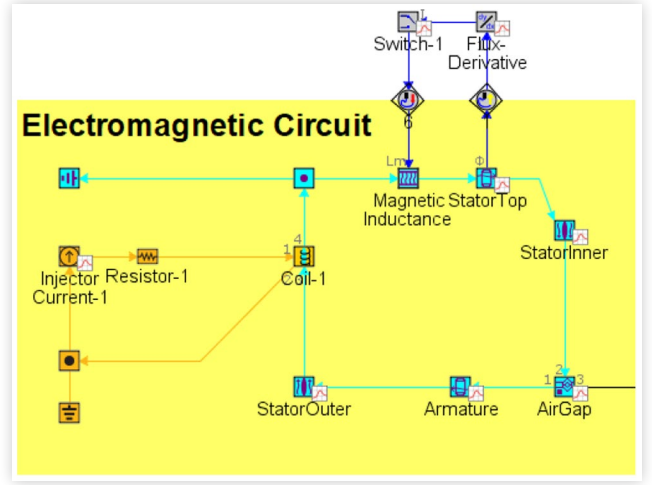
$$\dot{m} = \sum_{j=1}^n \dot{m}_j \quad (9)$$

$$\dot{p} = \gamma \cdot p \cdot \frac{\dot{m}}{m} + \frac{R}{V \cdot C_v} \left(\left(\sum_{j=1}^n \dot{m}_j h_j \right) - \dot{m} h \right) \quad (10)$$

$$\dot{T} = \frac{1}{C_p \cdot m} \left[\left(\sum_{j=1}^n \dot{m}_j h_j \right) - \dot{m} h + \dot{p} V \right] \quad (11)$$

Where C_p is the constant pressure specific heat, C_v the constant volume specific heat, h the specific enthalpy, V the volume and the subscript j indicate all the incoming and outgoing flows.

FIGURE 5 Representation of the electromagnetic circuit model in GT-Suite. The 'AirGap' element computes the resulting electromagnetic forces that the solenoid applies on the pintle.



The electromagnetic circuit includes only a simplified representation of the solenoid because injector current is imposed. The equivalent electromagnetic circuit (Figure 5) was created using conductors, inductors and a simplified armature model based on the work done in [10]. More detailed modeling of the electric circuit and the EM coupling with the injector equations of motion has been done, but it leads to a more complex model with a significantly greater number of parameters to calibrate [2, 3, 17]. By imposing the injector current, the interdependence of needle lift with instantaneous coil inductance and injector current can be ignored, thus enabling the use of a simplified injector driver circuit model [2, 3]. A control logic was used to adjust the magnetic inductance depending on whether the coil was charging or discharging in order to simulate the hysteresis-like response that can be observed in the magnetic hysteresis (B-H) curves.

Although mathematical models for all three primary injector components and suitable numerical methods had been identified, the choice was made to employ the commercial simulation software GT-Suite for the final model implementation. This decision was based on the advantages it offered, which outweighed any potential drawbacks. To integrate the resulting model over time, the software's built-in Runge-Kutta explicit method was utilized with good stability results.

Model Calibration Process

The model is meticulously calibrated to align with experimental data through a systematic three-step process:

1. **Electromagnetic constants and initial damping coefficient:** The focus in this initial stage is placed on tuning a reduced set of parameters in the model to match experimental data. Specifically, charging inductance, discharging inductance, and damping coefficients. Experimental injector pintle lift data recorded under "dry" conditions where the injector

inlet is unpressurized, is used as a reference. Imposing the experimental injector current profile as the only input to the model, an NSGA-II genetic algorithm is employed to minimize the error function between the experimental and model-predicted pintle lift.

2. **Flow path:** In this step, the goal is to obtain an accurate estimate of average flow and the forces stemming from fluid-structure interaction (FSI) that act on the pintle. To accomplish this, the flow path is discretized into a series of 0D and 1D flow elements that closely resemble the injector geometry. The experimentally recorded lift profiles and pressures upstream the injector gathered under various conditions, including different injector pulse-width durations and air pressures, are imposed to the pintle and injector inlet respectively. Initially estimated flow discharge coefficients are iteratively tuned by means of an NSGA-II genetic to refine the model until the disparity between the experimental and model-predicted average mass flow rates reaches a minimum.
3. **Final adjustments:** After completing the initial two steps, where a significant portion of the pintle's motion and flow characteristics were captured, a final refinement step is carried out. At this point, the model takes as inputs the current profile and air pressures measured upstream the injector. The local damping coefficients and seat stiffnesses are manually tuned until the amplitude and phase of the pintle bouncing are as close as possible to the experimental data while retaining good agreement with the overall lift profile. Finally, an NSGA-II genetic algorithm is used to further enhance this fit.

Results and Discussion

Experimental Results

Effect of driver voltage on the current and lift: In the first round of experimentation, the injector is run “dry” i.e. no air is used to tune the initial model for physical and electromechanical characteristics of the injector. For a fixed pulse width of 2.0ms, the voltage has negligible impact on the peak current recorded, but current rise rate increases with voltage (Figure 6). This higher rise rate during the earlier portion of the injection pulse becomes noticeable in the injector lift, initiating earlier, as seen in Figure 7. Reducing the injector delay to maximum lift and thus maximum rate of injection is critical at higher speeds and can push the non-linear region of the injector to shorter pulse-widths. Consideration of these advantages should be balanced by the increased complexity of the injector driving circuit.

The closing event happens roughly at the same time and with a similar characteristic bouncing irrespective of the voltage level selected (Figure 7). It is also worth noting that the system is more sensitive to this difference for voltages below 18V, point at which any additional increase in voltage starts to offer diminishing returns. No significant differences were noticed on the opening bouncing. The first event on

FIGURE 6 Influence of driver voltage on injector current profile. Increasing to the 24V reduces the time to reach peak current by half.

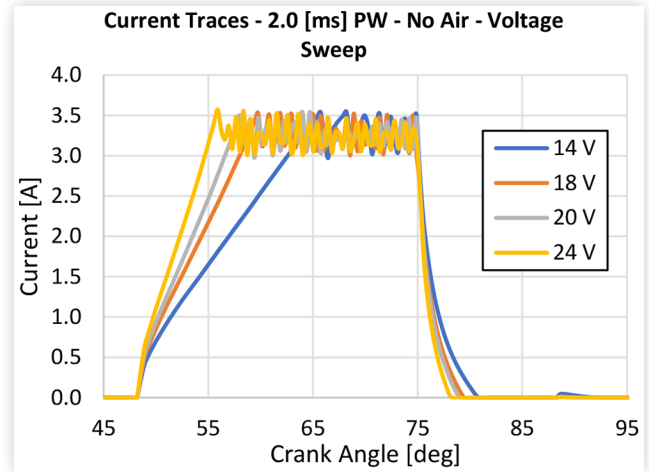
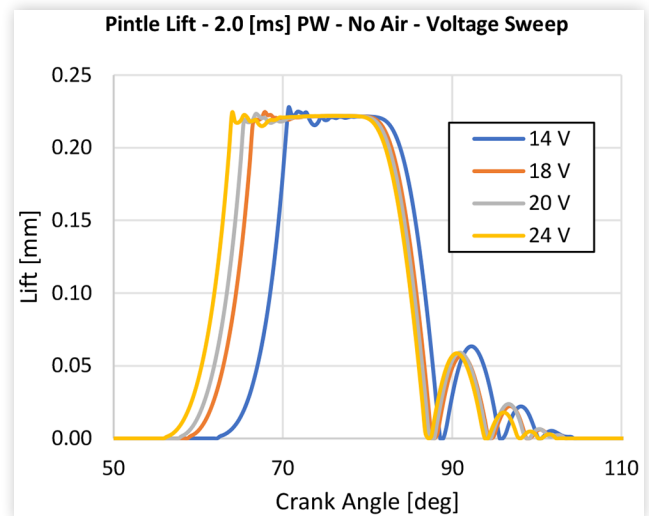


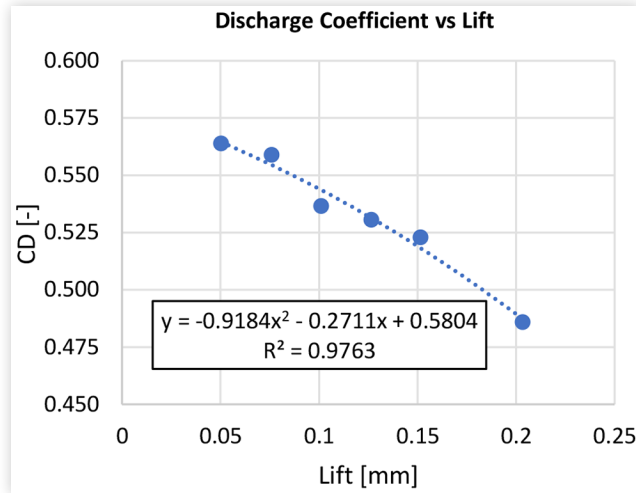
FIGURE 7 Effect of driver voltage on pintle lift profile. Faster currents from higher voltages results in a reduction of injector opening delay. Above 18V begins saturate this effect.



pintle rebound was found to be roughly one quarter of the nominal lift, again emphasizing the importance of capturing the injector pintle dynamics. This large magnitude of pintle bounce has been seen in other studies looking at gaseous fuel injectors. It has been suggested that this behavior isn't typically seen with injectors using liquid fuel due to the greater viscous damping provided by the fuel on the motion of the pintle [2, 3].

Static CD Estimation: To determine static discharge coefficient the injector maximum lift is imposed by a set screw, while the coil is energized with 2.5 amps. From sweeping air pressure and recording mass flows, static discharge coefficients were plotted versus needle lift seen in Figure 8. This observed experimental trend is similar to what can be found in literature for poppet valves [16]. Discharge coefficients showed higher values for lower lifts, with the peak value

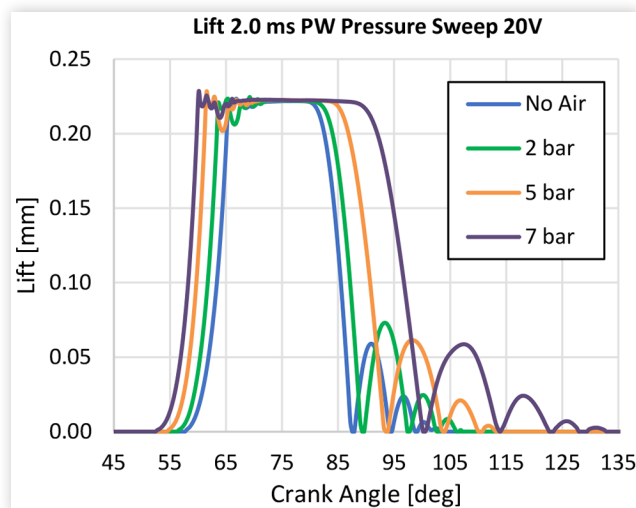
FIGURE 8 Experimentally determined discharge coefficients shows a similar trend found in literature to poppet valves



slightly below 0.57 at 50 microns of lift and the lowest value slightly above 0.48 at peak lift of 220 microns.

Effect of working fluid pressure on pintle lift and current: With static CDs and “dry” injector dynamics characterized, we introduce the influence of fluid-structure interaction by supplying air in typical injector operation. For a fixed voltage and pulse width, working fluid pressure has a very clear impact on the pintle lift profile seen in (Figure 9). Higher pressures follow a similar trend to higher driver voltages, creating earlier and faster injector opening. The same pressure sweeps were conducted at higher driving voltages, yet there was no visible influence on injector current. In the closing phase, the higher air pressures hinder the closing of the injector. Bouncing behavior is similar, however duration of the bounces is longer at higher pressures. While the higher pressures may be beneficial for spray penetration, injector

FIGURE 9 Influence of air pressure on pintle lift. Higher pressures reduce opening delay and also extend the time the pintle spends at maximum lift.



rebound could cause detrimental effects through unwanted reinjections of fuel. The use of voltage reversal would be required in order to dampen these effects. It should be noted that in this experimental set-up there is a fixed pressure differential between the upstream injector and the discharge area. In the final application, the design of air supply may vary pressure considerably relative to the instantaneous engine chamber pressures.

Modeling Results

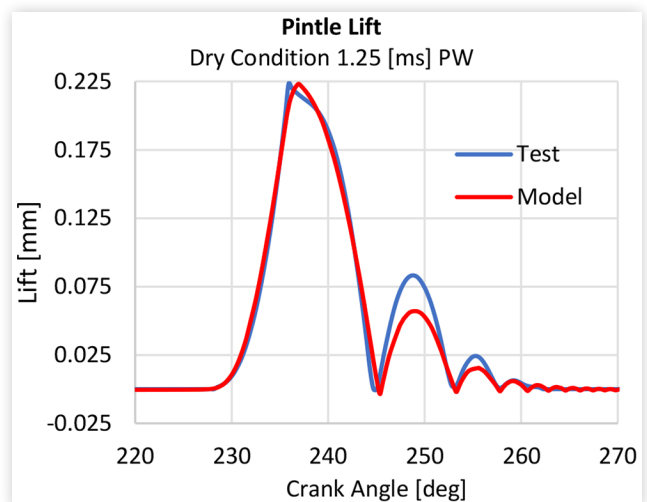
In the initial stage of the model calibration process, a need to increase the local damping constants significantly was observed. Specifically, the damping constants near the upper seat required a tenfold adjustment, while those near the lower seat warranted a twentyfold increase. These adjustments were expected and can be attributed to differences in seat geometry between the upper and lower seats. The upper seat's larger crevice area results in higher viscous damping as the pintle approaches the end stops, a phenomenon even apparent during 'dry' injector runs (i.e., without pressurized working fluid).

Regarding the tuning of the electromagnetic constants, it was determined that the charging inductance needed to be approximately five times greater than the discharging one in order to more closely match the system response.

After the initial model setup, “dry” behavior was very well captured. Figure 10 illustrates a comparison between the model's predictions and the experimental data, showcasing progress in fine-tuning the model.

For the flow path calibration, the initial approach followed the same procedure for poppet valves in internal combustion engines, in which a series of static CDs are obtained versus Lift-to-Diameter (L/D) ratio at different pressure ratios. It is assumed that the transient flow process is a series of quasi-steady states and therefore it should be possible to get a good

FIGURE 10 Model matching at dry conditions (i.e. no air pressure) at 1.25 ms injector pulse width. Bouncing phasing is well matched, although small discrepancies with the experimental data (blue) are still visible.



match using discharge coefficients predicted by the CD vs L/D curve [16]. This strategy did not provide a good match with flow, as the difference between behavior of transient and quasi-steady flow provided fundamentally different CD trends. The authors suspect that this is related to both the transient nature of the flow and the very low L/D ratio (~ 0.035). Other authors [18] have observed similar challenges to the quasi-steady assumption of the flow process through a poppet valve. An alternative method based on finding a constant CD as a function of the injector lift time area (LTA) was proposed after observing some trends in the data (Figure 11). Normalized CDs increased with higher lift time areas up to roughly a value of 0.9, in which all the data sets collected at different pressures showed similar asymptotic behavior.

Equation (2) is used to calculate the injector's Lift Time Area (LTA)

$$LTA = \int_{t_0}^{t_c} L_i(t) \cdot dt \quad (2)$$

Where t_0 is the time of start of the injector opening, t_c is the injector closing time, after the bouncing events, and L_i the instantaneous pintle lift.

While this method demonstrated a superior fit to average flow rates (as depicted in Figure 12) at a very low computational cost, it falls short of capturing the full complexity of the flow. Nevertheless, it aligns closely with the primary objective of this study, which is to estimate the forces exerted by the fluid on the pintle. For more precise instantaneous flow predictions, a detailed 3D-CFD model coupled with this injector pintle dynamics model should be employed.

The full model was constructed by incorporating the tuned parameters obtained in the previous two steps. Utilizing only the injector current signal and the working fluid properties upstream and downstream of the injector as inputs, the resulting model can accurately predict the instantaneous pintle lift under a variety of conditions as well as the average

FIGURE 11 Normalized injector nozzle CD as a function of normalized pintle lift time area

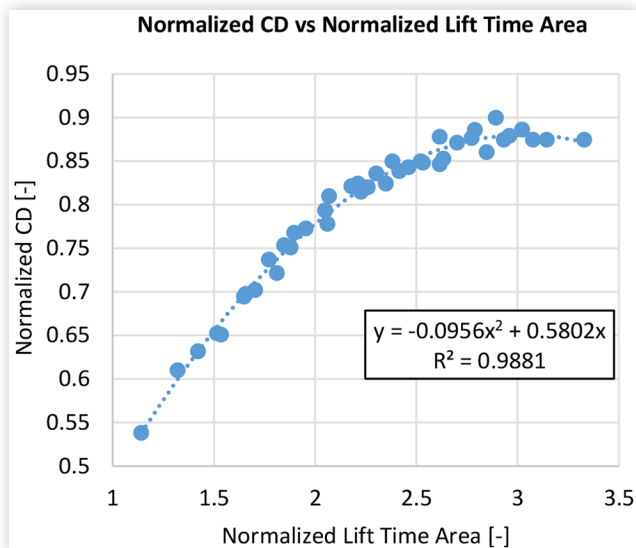


FIGURE 12 Comparison of the average flow rates predicted by the model using the lift time area approach (dashed lines) to the experimental data (solid lines) under different working fluid conditions.

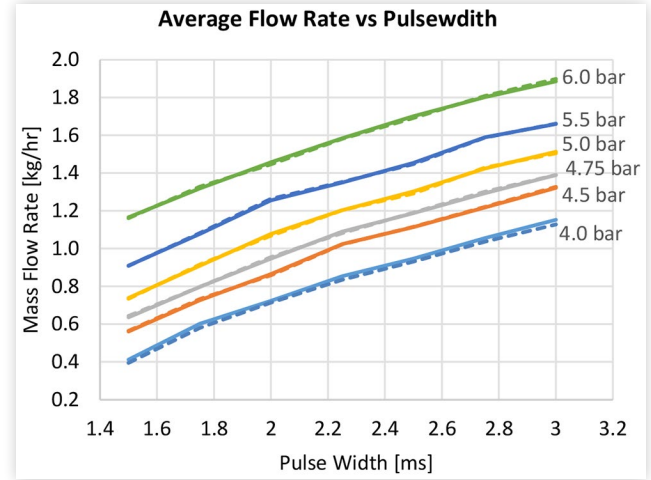
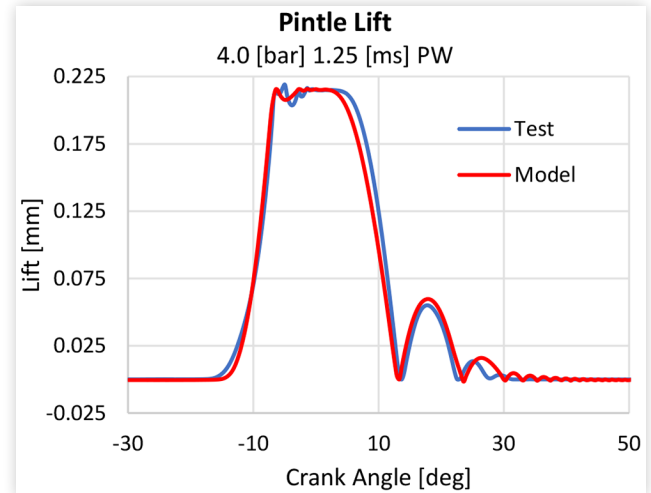


FIGURE 13 Comparison of test data to predicted model using an imposed injector current shows good agreement. Best agreement is found at low to intermediate pressures and medium to long pulse widths



flow rates. Figure 13 provides a visual demonstration of the remarkable alignment between the model's pintle lift predictions and experimental data.

Summary and Conclusions

In typical ICE mixture formation research, injector pintle lift is imposed in order to focus on the spray. It is known how big of an influence pintle position has on the spray, and therefore any inaccuracies in this would lead to incorrect model predictions. This study begins the mixture formation research for an outward opening pintle valve by integrating pintle lift data into a GT-Suite model, with the goal of both gaining insight on the

system response to different inputs and provide more accurate boundary conditions for detailed spray modeling. Alignment between experiments and model development enables the study of different contributions of EM and FSI forces on the injector dynamics. Development of the experimental and analytical procedures allowed for further understanding the influence of operating parameters such as driver voltage, working fluid pressure, and pulse-width (included in the current signal) on pintle dynamics. A simple multi-physics model was developed using commercial modeling software, to predict pintle lift using injector current signal and working fluid properties as inputs. This work is the first of several steps required to fully characterize the mixture formation using an outward opening pintle valve. A summary of the conclusions are listed below:

- Driver voltage has a significant effect on needle lift and current rise rates. Careful design of driver circuitry should be considered for improved injector control.
- In the case of an outward opening pintle injector, the working fluid pressure has a noticeable effect on the lift profile. Higher pressures cause the pintle to open faster and dwell longer at maximum lift.
- The use of statically determined discharge coefficients along with the quasi-steady flow assumptions did not yield satisfactory results. While this has been reported in other studies [18] authors consider more research is necessary. In the interim, an alternative method based on lift time area was proposed and found to have an excellent fit with experimental data.
- A simple yet effective model capable of accurately predicting the pintle lift profile and average flow rates using the injector current signal and working fluid pressure upstream was implemented.
- Understanding how the system reacts to different inputs allows for more accurate control strategies that can result in better engine efficiency guiding engine testing through modeling.

In the course of this research, we have identified additional opportunities for improvement. These include a more comprehensive contact model, a more thorough representation of the electromagnetic circuit and adjustments to the flow path model to mitigate uncertainties. Future directions will include experimental spray characterization and extending our simulations to 3D CFD, while enhancing the quality and depth of the electromagnetic model. One avenue of exploration is considering the needle as an elastic multibody system, which may offer a more accurate representation. Further investigation of the discrepancies between the quasi-steady flow assumption for CD methodology is required. Another model improvement would be coupling the dynamic model with CFD code to obtain a fully predictive spray model.

References

1. Powell, C.F., Kastengren, A.L., Liu, Z., and Fezzaa, K., "The Effects of Diesel Injector Needle Motion on Spray Structure," 2011, 012802.
2. Cammalleri, M., Pipitone, E., Beccari, S., and Genchi, G., "A Mathematical Model for the Prediction of the Injected Mass Diagram of a SI Engine Gas Injector," *Journal of Mechanical Science and Technology* 27 (2013): 3253-3265.
3. Pipitone, E., Beccari, S., Cammalleri, M., and Genchi, G., "Experimental Model-Based Linearization of a SI Engine Gas Injector Flow Chart," *Strojniški vestnik-Journal of Mechanical Engineering* 60, no. 11 (2014): 694-708.
4. Berger, S., Wegmann, T., Meinke, M., and Schröder, W., "Large-Eddy Simulation Study of Biofuel Injection in an Optical Direct Injection Engine," SAE Technical Paper 2020-01-2121 (2020), <https://doi.org/10.4271/2020-01-2121>.
5. Mata, C., Rojas-Reinoso, V., and Soriano, J.A., "Experimental Determination and Modelling of Fuel Rate of Injection: A Review," *Fuel* 343 (2023): 127895.
6. Sim, J., Badra, J., Elwardani, A.E., and Im, H.G., "Spray Modeling for Outwardly-Opening Hollow-Cone Injector," 2016.
7. Srinivasan, K.K., Agarwal, A.K., and Krishnan, S.R., in: Mulone, V. (Eds), *Natural Gas Engines. Energy, Environment, and Sustainability*, (Singapore: Springer, 2019).
8. Atef, N., Badra, J., Jaasim, M., Im, H.G. et al., "Numerical Investigation of Injector Geometry Effects on Fuel Stratification in a GCI Engine," *Fuel* 214 (2018): 580-589.
9. Badra, J.A., Sim, J., Elwardany, A., Jaasim, M. et al., "Numerical Simulations of Hollow-Cone Injection and Gasoline Compression Ignition Combustion with Naphtha Fuels," *Journal of Energy Resources Technology* 138, no. 5 (2016): 052202.
10. Payri, R., Salvador, F.J., Martí-Aldaraví, P., and Martínez-López, J., "Using One-Dimensional Modeling to Analyze the Influence of the Use of Biodiesels on the Dynamic Behavior of Solenoid-Operated Injectors in Common Rail Systems: Detailed Injection System Model," *Energy Conversion and Management* 54, no. 1 (2012): 90-99.
11. Deshmukh, A.Y., Giefer, C., Goeb, D., Khosravi, M. et al., "A Quasi-One-Dimensional Model for an Outwardly Opening Poppet-Type Direct Gas Injector for Internal Combustion Engines," *International Journal of Engine Research* 21, no. 8 (2020): 1493-1519.
12. Blair, G., *Design and Simulation of Four-Stroke Engines* (SAE International, 1999).
13. Salvador, F.J., Gimeno, J., De la Morena, J., and Carreres, M., "Using One-Dimensional Modeling to Analyze the Influence of the Use of Biodiesels on the Dynamic Behavior of Solenoid-Operated Injectors in Common Rail Systems: Results of the Simulations and Discussion," *Energy Conversion and Management* 54, no. 1 (2012): 122-132.
14. Plamondon, E. and Seers, P., "Development of a Simplified Dynamic Model for a Piezoelectric Injector Using Multiple Injection Strategies with Biodiesel/Diesel-Fuel Blends," *Applied Energy* 131 (2014): 411-424.
15. Winterbone, D.E. and Pearson, R.J., *Theory of Engine Manifold Design: Wave Action Methods for IC Engines* (London: Professional Engineering Publishing, 2000).
16. Heywood, J.B., *Internal Combustion Engine Fundamentals* (McGraw-Hill Education, 2018).

17. Brauer, J.R., *Magnetic Actuators and Sensors* (John Wiley & Sons, 2006).
18. Winroth, P.M., Ford, C.L., and Alfredsson, P.-H., "On Discharge from Poppet Valves: Effects of Pressure and System Dynamics," *Experiments in Fluids* 59 (2018): 1-15.

Acknowledgments

This material is based upon work supported by, or in part by, the U. S. Army Research Laboratory under contract agreement W911NF2190005. The views and opinions of authors expressed herein do not necessarily state or reflect those of the United States Government or any agency thereof.

Copyright

The U.S. has a copyright license in this work pursuant to an Other Transaction Agreement. The United States Government retains, and Licensee acknowledges that the United States Government retains, a non-exclusive, paid-up, irrevocable, world-wide license to publish or reproduce the published form of this Work, or allow others to do so, for United States Government purposes.

Definitions/Abbreviations

CFD - Computational Fluid Dynamics

CD - Discharge Coefficient

DOE - Design of Experiments

EM - Electromagnetics

FSI - Fluid-Structure Interaction

NSGA-II - Non-Dominated Sorted Genetic Algorithm

PW - Pulse-width

RBD - Rigid Body Dynamics

ROI - Rate of injection